How vial geometry variability influences heat transfer and product temperature during freeze-drying

Bernadette Scutella, Stéphanie Passot, Erwan Bourlés, Fernanda Fonseca, Ioan-Cristian Trelea

How vial geometry variability influences heat transfer and product temperature during freeze-drying

Authors: BERNADETTE SCUTELLA[1,2], STEPHANIE PASSOT[1], ERWAN BOURLES[2], FERNANDA FONSECA[1], IOAN CRISTIAN TRELEA[1]

[1] UMR GMPA, AgroParisTech, INRA, Université Paris Saclay, 78850 Thiverval-Grignon, France

[2] GSK Vaccines, Rixensart, Belgium

ABSTRACT: Vial design features can play a significant role in heat transfer between the shelf and the product and, consequently, in the final quality of the freeze-dried product. Our objective was to investigate the impact of the variability of some geometrical dimensions of a set of tubing vials commonly used for vaccine production on the distribution of the vial heat transfer coefficients (K_v) and its potential consequence on product temperature. Sublimation tests were carried out using pure water and eight combinations of chamber pressure (4 to 50 Pa) and shelf temperature (-40 °C and 0 °C) in two freeze-dryers. K_v values were individually determined for 120 vials located in the center of the shelf. Vial bottom curvature depth and contact area between the vial and the shelf were carefully measured for 120 vials and these data were used to calculate K_v distribution due to variability in vial geometry. At low pressures commonly used for sensitive products (below 10 Pa), the vial-shelf contact area appeared crucial for explaining K_v heterogeneity and was found to generate, in our study, a product temperature distribution of approximately 2 °C during sublimation. Our approach provides quantitative guidelines for defining vial geometry tolerance specifications and product temperature safety margins.

Keywords: Freeze drying/lyophilization; amorphous; drying; vaccines; distribution; vial heat transfer coefficient; sublimation rate; vial design; inter-vial heterogeneity

INTRODUCTION

Nowadays, freeze-drying is an essential and valuable preservation method to ensure the long-term stability of the growing list of biopharmaceuticals such as antibodies, hormones, vaccines, therapeutics peptides and proteins. This method makes it possible to remove the majority of water at temperatures far below 0 °C (usually between -40 °C and -20 °C) by sublimation, the phase transition from ice to water vapor.[1]

Due to the really low temperature and pressure typically used, freeze-drying remains a time consuming process often difficult to control and scale-up. The US Food and Drug Administration has recently proposed a new regulatory philosophy to manage product quality: the Quality by Design (QbD) initiative. Quality will be no more tested into the product but designed into the process. The QbD approach is based on pre-defined quality targets and on a deep understanding of how formulations and process interact to influence critical quality attributes of pharmaceutical products.[2] In contrast to tablets, products intended to be freeze-dried are conditioned in their final packaging system (vial or syringe) before the process.[3] The vial thus directly influences the freeze-drying process and impacts final product quality.[4,5] Furthermore, since the capacity of a manufacturing freeze-dryer can easily reach 100 000 vials, ensuring uniform product quality attributes (potency of the active ingredient, residual moisture content, visual aspect of the freeze-dried cake) within the entire batch represents a real challenge. Any variation in the design of the packaging system or other parameters could result in product quality variation.

Product temperature is a key process parameter governing an important critical product quality attribute, the visual aspect of the freeze-dried cake, which in turn could influence the residual moisture, the stability of the active ingredient and the reconstitution time.[6] During the process the product temperature should be maintained below a critical value corresponding to the glass transition temperature in amorphous product.[3,7] However, the

product temperature profile cannot be directly controlled and depends on the process operating parameters (i.e., shelf temperature, chamber pressure) and on the heat transfer through the container (e.g., vial).[4,7,8] Knowledge of the heat transfer characteristics of the vial and the uniformity or non uniformity of this property within vial arrangement inside a freeze-dryer is thus essential to be able to predict final quality of the product batch. Several authors have reported that the heat transfer rate between the shelf and the product is dependent on the vial position on the shelf.[4,5,9–12] Pikal et al.[5] showed that the vials located at the periphery of the shelf exhibited sublimation rates 15% higher than vials located in the center. This phenomenon, referred to as "edge effect", has been ascribed to additional heat transfer by radiation from walls and doors.[4,5,8,9,11] The higher heat flow rate of these periphery vials could lead to product collapse due to increased product temperatures during the primary drying phase. Furthermore, Pisano et al.[10] recently observed a normal distribution in the vial heat transfer coefficient evaluated for vials located in the center of the shelf.

The design of the vial also strongly influences the heat transfer efficiency between the shelf and the product.[4,5,7,12–15] Considering that the vials are placed directly on the shelf, the heat flow transferred to the product can be described by three parallel mechanisms: conduction from the shelf surface to the vial *via* points of direct contact between the vial bottom and the shelf, conduction through the vapor entrapped in the vial bottom concavity and radiation.[5,8,12] Heat transfers *via* contact conduction and conduction through the gas are influenced, respectively, by the dimension of the contact area between the shelf and the vial and the depth of bottom curvature in which the gas is entrapped.[5,8,12] Several studies[13,16,17] have demonstrated that the vial bottom curvature limits the heat transfer and, thus, the sublimation flow rate that determines the duration of the primary drying. The concavity of the vial bottom limits the direct surface contact between the vial and the shelf, accounting for most of the resistance to conductive heat transfer.[14,16] In pharmaceutical freeze-drying conditions, contact

conduction is more efficient than gas conduction, and an increase in the contact area leads to a significant increase in the total heat transfer.[5,14]

Our objective was to quantitatively investigate the role of vial geometry distribution on heat transfer heterogeneity and subsequently on product quality by predicting product temperature distribution during the primary drying step induced by variability in vial dimensions. Proposing an approach to understand how vial design and operating conditions interact to influence product quality is completely in the scope of the QbD approach.

In the present study, only vials located in the center of the shelf and surrounded by other vials in the same conditions were considered so as to avoid any heterogeneity due to the additional border heat transfer. The analysis of the heterogeneity was conducted in terms of vial heat transfer coefficient (K_v) distributions. Based on theoretical analysis,[5,8,12] attention was focused on the role of two vial dimensions, the bottom curvature depth and the contact area between the bottom vial and the shelf. Two shelf temperatures (-40 °C and 0 °C) and six chamber pressures (4, 6, 9, 15, 40 and 50 Pa) were tested in two freeze-dryer pilot plants of similar shelf emissivity to assess the impact of these operative parameters on the heat transfer heterogeneity among central vials. Finally, as example of practical application of our work for assessing the pharmaceutical product quality, the impact of the central vial K_v variability on product temperature was evaluated. Product temperature distributions for a 5 % sucrose solution were calculated from the simulated K_v distributions based on the vial geometry for several operating conditions.

MATERIALS AND METHODS

Materials

Siliconized glass tubing vials (3 mL) were provided by Müller + Müller (Holzminden, Germany). These vials are routinely used in commercial manufacturing. Distilled water was used throughout the experiments.

Two pilot scale freeze-dryers differing mainly by their size, the type of valve connecting the drying chamber to the condenser and their age were used for this study:

- a LyoVac GT6 (Finn-Aqua Santasalo-Sohlberg SPRL, Brussels, Belgium), referred to as LYO A. It included 5 shelves with an area of 0.14 m² each, a distance between shelves of 56 mm, a drying chamber volume of 0.061 m^3 and a butterfly valve between the chamber and the condenser.

- an Epsilon 2-25D (Martin Christ Gefriertrocknungsanlagen GmbH, Osterode am Harz, Germany), referred to as LYO B. It included 7 shelves with an area of 0.27 m² each, a distance between shelves of 55 mm, a drying chamber volume of 0.38 m^3 and a mushroom valve between the chamber and the condenser.

The pressure in the freeze-dryer chamber was monitored by a capacitive manometer. Since it was not technically possible to install thermocouples in the drying chamber of the two freeze-dryers, Tempris wireless sensors (IQ Mobil Solution GMbH, Holzkirchen, Germany) were positioned in the bottom center of selected vials (Figure 1) to record ice temperature during the experiments. The obtained signal was used to define the sublimation starting point.

Ice sublimation experiments

All experiments were performed using a 1.8 mL fill volume of distilled water (filling height: 11 mm). No stopper was inserted into the vial neck. The middle shelf was fully covered by filled vials for all runs, corresponding to a total of 540 vials in LYO A and 950 vials in LYO B. Bottomless trays were used.

The vials were quickly loaded on the pre-cooled shelf at -50°C. The presence of a dry laminar flow in front of the freeze-dryer door made it possible to control the air relative humidity and thus to limit condensation on the shelves. After a freezing step of 2 hours, the pressure was decreased and the shelf temperature was increased by 1 °C/min. Experiments were carried out at 4, 6, 9, 15, 40 and 50 Pa with a shelf fluid inlet temperature of 0 °C, and at 4 and 6 Pa with a shelf fluid inlet temperature of -40 °C. The run performed at 0 °C and 6 Pa was repeated three times. The cycles were run long enough to dry up to 20-25 % of the initial fill volume. Subliming a larger quantity of ice could lead to loss of contact between the vial and the ice, introducing uncertainty in the analysis.

The sublimation rate $\dot{m}$ was measured gravimetrically for each vial and calculated as the mass loss divided by the period of sublimation. A total of 100 vials, placed in the centre of the shelf and surrounded by other vials in the same conditions, were individually weighed before and after the experiment on a precision scale (± 0.001 g; Mettler Toledo, Zaventem, Belgium). Sublimation time was measured from the moment when shelf temperature exceeded product temperature, meaning that there was a net heat flux from the shelf towards the vials. The arrangement of the weighed vials within the shelves is shown in Figure 1 for the two freeze-dryers.

Measurement of emissivity of the vial and of the shelf

Emissivity measurements were performed by Themacs Ingénierie (Champs sur Marne, France). The glass vial emissivity was determined using a Fourier transform infrared spectrophotometer (Frontier, Perkin Elmer, Roissy, France) equipped with a Pike© integrant sphere (Pike Technologies, Fitchburg, WI, USA). The measured emissivity varied from 0.78 to 0.80 within the range of temperatures tested (from -48 °C to 27 °C). Thus, a constant value

153 corresponding to the average observed product temperatures (between -48 to -24 °C) was
154 used in the data analysis, as reported in Table 1.
155 The shelf emissivity was measured using the emissometer EM-2, making it possible an in situ
156 measurement.[18] The emissivity value of the shelves of LYO B was 0.18 ± 0.06 (Table 1).
157 Measurements were carried out on several pilot and production freeze-dryers and shelf
158 emissivity values in the range of 0.18-0.3 were obtained. Considering the relative standard
159 deviation of the method (0.06), the measured values are in agreement with values reported in
160 literature.[5]
161
162 **Dimensional analysis of a batch of vials**
163 The dimensions of 120 vials were precisely measured by the specialized company
164 Precis&Mans (Le Mans, France) using the micrometer Mitutoyo 3D (Mitutoyo Europe
165 GmbH, Neuss, Germany). The following geometrical parameters were determined with a
166 precision of 0.003 mm: the inner and outer bottom radius and the maximum bottom curvature
167 depth. These values were used to calculate additional vial dimensions: outer and inner vial
168 bottom area, vial shelf contact area (A_c) (named radius-based contact area in Table 1) and
169 mean bottom curvature depth (l) (Appendix).
170 Furthermore, the vial-shelf contact area was also estimated using the imprint method
171 proposed by Kuu et al.[17] and Hibler et al.[4] The vials were gently placed on an inkpad and then
172 on a sheet of white paper. ImageJ v.1.49 software (National Institutes of Health, Bethesda,
173 MD, USA) was used for the determination of the vial-shelf bottom contact area in pixels from
174 the imprint images. The scale factor of pixels in mm^2 was determined by evaluating the
175 number of pixels of a black shape of known area and was equal to 0.0153 mm^2 $pixel^{-1}$. The
176 mean value and the relative standard deviation of these geometrical dimensions are reported
177 in Table 1. The two methods used for evaluating the vial-shelf contact area gave similar mean

values: 16.7 mm² for the imprint method and 17.8 mm² for the dimensional analysis. However, the coefficient of variation of these methods appeared different and significantly higher for the imprint method (23.9 % versus 12.0 % for the dimensional analysis). The values of contact area determined using this latter method were selected for the analysis considering that this method better accounts for intimate contact between vial and shelf.

THEORY AND DATA ANALYSIS

Evaluation of the vial heat transfer coefficient K_v based on experimental data

As widely reported in literature,[4,5,8,12] the vial heat transfer coefficient K_v was calculated using the following equation:

$$K_v = \frac{\dot{Q}}{A_b(T_s - T_b)} = \frac{\Delta H\, \dot{m}}{A_b(T_s - T_b)} \qquad \text{Equation 1}$$

where $\dot{Q}$ is the heat flow received by the vial, A_b is the outer vial bottom area, T_s is the average temperature between the inlet and outlet shelf fluid temperatures, T_b is the bottom product temperature, ΔH is the latent heat of sublimation and $\dot{m}$ is the sublimation rate.

Since it was not possible to implement thermocouples in the freeze-dryer pilot plant to have a precise measurement of the product temperature, T_b was theoretically determined as:

$$\dot{Q} = \frac{\lambda_{ice}}{L_{ice}} A_{in}(T_b - T_i) \qquad \text{Equation 2}$$

where λ_{ice} is the ice thermal conductivity, A_{in} is the inner bottom area of the vial, L_{ice} is the ice thickness and T_i is the ice-vapor interface temperature. The ice thickness was estimated as

the mean between the initial and final ice thickness values (calculated using the amounts of initial and sublimed ice).

No stopper and pure water were used in this study in order to assume that the partial pressure of vapor at the sublimation interface was equal to the chamber pressure. The temperature at the ice-vapor interface T_i was thus calculated as a function of the interface pressure P_i using the Clausius-Clapeyron relation:[19]

$$T_i = \frac{6139.6}{28.8912 - \ln(P_i)} \quad \text{Equation 3}$$

The T_b value calculated was compared to the product temperature value given by the Tempris probe and an excellent agreement between experimental and theoretical data was observed.

Theoretical description of the vial heat transfer coefficient K_v

The main objective of this work was to quantify the impact of vial dimensions distribution on heat transfer variability and its resulting consequence on product temperature. To this end, the vial heat transfer coefficient need to be theoretically expressed in function of specific vial dimensions.

The vial heat transfer coefficient K_v can be described as the sum of three contributions:[5,8,12]

$$K_v = K_c + K_g + K_r \quad \text{Equation 4}$$

where K_c represents the thermal contact conduction between the shelf and the vial *via* the direct contact area, K_g the thermal conduction through the gas entrapped in the vial bottom curvature and K_r the thermal radiation between the vial and the top and bottom shelves.

Heat transfer by thermal contact conduction K_c

The expression of K_c has been discussed in the literature by only a few authors.[16,17] Kuu et al.[17] proposed an evaluation of this parameter and showed that the larger the contact area is, the larger the value of the contact conduction coefficient will be. Thus, K_c can be assumed to be proportional to the contact area (A_c, evaluated by the imprint test method) through an empirical constant (C_1):

$$K_c = C_1 A_c \qquad \text{Equation 5}$$

Heat transfer by conduction through the gas K_g

The coefficient K_g, representing the contribution of the conduction through the gas in K_v, can be expressed as:[5,12]

$$K_g = \frac{C_2 P_C}{1+\frac{C_2 l}{\lambda_{amb}} P_C} \qquad \text{Equation 6}$$

where P_C is the chamber pressure, λ_{amb} is the molecular conductivity of the water vapor at ambient pressure, l is the mean vial bottom curvature depth calculated as reported in the Appendix, and the coefficient C_2 is equal to:

$$C_2 = \Lambda_o \frac{\alpha_c}{2-\alpha_c} \left(\frac{273.15}{T_{gas}}\right)^{0.5} \qquad \text{Equation 7}$$

where Λ_o is the free molecular heat conductivity of the gas at 0 °C, T_{gas} is temperature of the gas participating to heat conduction, calculated as average between the product temperature

at the sublimation interface and the shelf temperature values,[12] and α_c is the accommodation coefficient.

Heat transfer by thermal radiation K_r

The heat transfer by radiation between the shelf and the vial $\dot{Q}_r^{shelf}$ can be described by the Stephen-Boltzmann equation:[5,8,20]

$$\dot{Q}_r^{shelf} = A_r \mathcal{F} \sigma ({T_s}^4 - {T_b}^4) \quad \text{Equation 8}$$

where A_r is the area exposed to the radiation from the shelves to be considered equal to the vial bottom area A_b, $\mathcal{F}$ is the visualization factor and σ the Stephan-Boltzman constant. After mathematical rearrangement, Equation 8 can be expressed as:

$$\dot{Q}_r^{shelf} = A_r \mathcal{F} \sigma \left({T_s}^4 - {T_b}^4\right) = A_b \mathcal{F} \sigma (T_s + T_b)(T_s^2 + T_b^2)(T_s - T_b) \quad \text{Equation 9}$$

Thus, the heat transfer coefficient K_r for thermal radiation can be defined as:

$$K_r = \mathcal{F} \sigma (T_s + T_b)(T_s^2 + T_b^2) \quad \text{Equation 10}$$

During the process, central vials are affected by two different radiative heat transfer contributions: between (i) the shelf below the vial and the vial bottom, and (ii) the shelf above the vial and the top of the vial.[5,8,12] Hence, the visualization factor will be the sum of two terms:

$$\mathcal{F} = \mathcal{F}_b + \mathcal{F}_{top} \quad \text{Equation 11}$$

The visualization factor at the bottom of the vial $\mathcal{F}_b$ can be evaluated considering the definition proposed by Bird et al.[20] and Pikal[8] for the heat transfer by radiation between parallel surfaces:

$$\mathcal{F}_b = \frac{1}{1+\left(\frac{1}{e_v}-1\right)+\left(\frac{1}{e_s}-1\right)} \quad \text{Equation 12}$$

where e_v and e_s are the emissivities of the vial and shelf, respectively.

Considering vials located in the centre of the shelf and surrounded by other vials in the same conditions, it is possible to assume that (i) the vial area exposed to the top shelf is much smaller than the area of the shelf and (ii) the vial top does not receive radiations from the side walls of the chamber. Thus, the visualization factor between the top of the vials and the shelf $\mathcal{F}_{top}$ can be estimated equal to the emissivity of the vial:[5,8]

$$\mathcal{F}_{top} = e_v \quad \text{Equation 13}$$

In agreement with the literature, the visualization factor at the vial top (equal to 0.78; Table 1) is higher than the one at the vial bottom (equal to 0.16; Table 1).[5]

Dependence of the vial heat transfer coefficient on vial geometry

Equations 4, 5 and 6 were combined to highlight the dependence of K_v on the contact area (A_c), and bottom curvature depth (l):

$$K_v = C_1\, A_c + K_r + \frac{C_2\, P_c}{1+\frac{l}{\lambda_{amb}} C_2\, P_c} \quad \text{Equation 14}$$

299 The term K_r was calculated from Equations 10-13 for each experimental condition.
300 Coefficients C_1 and C_2 were determined by fitting Equation 14 in a least-squares sense to
301 experimental K_v values determined by the gravimetric method. Calculations were performed
302 with Matlab R2014b software equipped with the Statistics Toolbox (The Mathworks Inc.,
303 Natick, MA, USA). The bottom curvature depth l and contact area A_c were evaluated from
304 dimensional analysis of the vial and imprint test, respectively.
305
306 **Calculation of K_v distributions based on vial geometry**
307 Two vial dimensions influence heat transfer: the contact area (A_c) and the mean bottom
308 curvature depth (l). The absence of correlation between the two geometrical dimensions l and
309 A_c was verified by calculating the correlation factor together with its statistical significance
310 (p-value > 0.5). It was thus possible to independently evaluate the impact of those parameters
311 on K_v. Using Equation 14, three K_v distributions based on vial dimension variations were
312 simulated: (i) curvature-based (l in Equation 14); (ii) contact area-based (A_c in Equation 14);
313 and (iii) their combination. The curvature-based K_v distribution was obtained by evaluating
314 Equation 14 with the 120 measured values of the mean bottom curvature depth (l), while the
315 contact area was maintained constant at its mean value. The contact area-based K_v
316 distribution was obtained by evaluating Equation 14 with the 120 measured values of the
317 imprint-based contact area (A_c), whereas the bottom curvature depth was maintained constant
318 at its mean value. Plugging both measured l and A_c values into Equation 14 gave the
319 combined contact area and curvature-based K_v distribution. The calculation was repeated for
320 all the studied chamber pressures and shelf temperatures. Chi-square goodness-of-fit tests were
321 performed on the simulated K_v distributions, establishing that the sample data were consistent
322 with a normal distribution at a 0.05 significance level.
323

Simulation of the product temperature distributions using the K_v distribution

Product temperature distributions were obtained from the calculated contact area and curvature-based K_v distribution. The product temperature was calculated for a 5 % w/w sucrose solution, considering a shelf temperature of -25°C and four chamber pressures (4, 6, 9, 15 Pa). Pressure at 40 and 50 Pa were not considered because the product temperature exceeds the glass transition temperature of the product at such high pressure (i.e., -32 °C for a 5 % w/w sucrose solution).[21] In the case of a real product, the mass flow rate can be expressed as reported by Pikal et al.[5]:

$$\dot{m} = \frac{(P_i - P_c)\, A_{in}}{R_p} \qquad \text{Equation 15}$$

where R_p represents the area-normalized product resistance. The value of R_p used for this simulation is reported in Table 1 and was considered for a dried layer thickness of 0.5 cm.[21] To simulate the product temperature distribution, the non-linear system composed of Equations 1-3 and 14-15 was solved for each pair of measured l and A_c values. Chi-square goodness-of-fit tests were performed on the product temperature distributions, demonstrating that the simulated data were compatible with a normal distribution at a 0.05 significance level.

RESULTS AND DISCUSSION

Impact of equipment on K_v

Vial heat transfer coefficient K_v of 100 vials located in the centre of the shelf was experimentally determined for different chamber pressures (4 to 50 Pa), shelf temperatures (-40 °C and 0 °C) and freeze-dryers (LYO A and LYO B). Figure 2 illustrates the evolution of the average value of K_v with pressure. Equation 14 was fitted with the experimental data and

the resulting coefficients C_1 and C_2 are presented in Table 2 for the data obtained in LYO A, LYO B and their combination. The accommodation coefficient α_c was also calculated from Equation 7, considering an average value of the gas temperature obtained under the different operating conditions tested (T_{gas} = -35 °C). The obtained values of the accommodation coefficient appear to be in agreement with data in literature.[8]

In Table 2, LYO A and LYO B exhibited a similar value of the C_1 coefficient that is related to the contact area coefficient K_c (Equation 5), but distinct values of the C_2 coefficient that is related to K_g (Equation 6). LYO B exhibited a slightly higher accommodation coefficient then LYO A, probably due to a different finish of the freeze-dryer shelf material.

When considering pressure values lower than 10 Pa (Figure 2), the K_v values obtained in the two freeze-dryer appeared similar. This result was confirmed also by Pisano,[12] who reported no significant difference in K_v value of central vials processed in a pilot and manufacturing freeze-dryer at a pressure of 10 Pa. For pressure value higher than 10 Pa, the influence of freeze-dryer configuration became significant with slightly higher values obtained in LYO B (Figure 2). At 50 Pa, the K_v value was approximately 8% higher in LYO B than in LYO A. Considering the different values of C_2 coefficient, the K_v difference between freeze-dryers at high pressure can thus be ascribed to the increased rate of heat transfer through the gas over the total heat flow. However, the physical origin of the differences in the pressure-dependent component of K_v remains unclear. Possible hypotheses include: (i) differences in the shelf surface finish that could induce differences in the gas-shelf heat transfer through the accommodation coefficient[8] (Equation 6-7) as well as (ii) differences in the gas convection conditions, a mechanism responsible for a small part of the pressure-dependent heat transfer.[22] These results suggest that small differences between devices might become more apparent at high pressures. When considering only vials not exposed to edge effect a cycle designed with low operating pressure (below 10 Pa) could therefore be more suitable for safe

scale-up. However the behavior of the edge vials located at the periphery of the shelf or in contact with metallic band need also to be considered and some elements were recently proposed by Pikal et al.[11] to investigate the impact of the freeze-dryer configuration.

Impact of chamber pressure and shelf temperature on K_v

As reported in the literature and shown in Figure 2, chamber pressure had a strong impact on K_v.[4,5,8,12,13,15] The vial heat transfer coefficient increased approximately four times between 4 and 50 Pa. At the vial bottom, the presence of the curvature limits the intimate contact between the shelf and the vial and create an empty space between the shelf and the vial that acts as an insulator.[13,16,17] At very low pressures typically used in the process, the heat transfer contribution by gas convection is usually neglected,[11] whereas the contribution of gas conduction has to be considered. This heat transfer mechanism, represented by the coefficient K_g, is dependent on the chamber pressure and increases when increasing pressure, as shown in Equation 6.[5,8,12,15] Figure 3 shows the relative contributions of K_c, K_r and K_g on the total K_v, calculated using the set C of the fitting coefficients reported in Table 2. The K_c and K_r contributions go from about 30 % at 4 Pa to 10 % at 50 Pa, whereas the K_g contribution goes from about 25 % at 4 Pa to 80 % at 50 Pa.

A moderate effect of shelf temperature on K_v was expected theoretically due to K_r (Equation 10) and to K_g through the gas temperature (Equations 6-7). Figure 4a displays the influence of shelf temperature on K_v. Differences in K_v values due to temperature remained within the standard deviation when considering pressure values lower than 10 Pa and when the contribution of K_g in the total K_v is moderate (around 25 %, Figure 3).

In order to clarify the impact of the shelf temperature, the contributions of the single coefficients K_c, K_r and K_g on K_v were calculated for two shelf temperatures (25 °C and -25 °C) and three chamber pressures (4, 6 and 50 Pa), as show in Figure 4b. The contact

399 conduction coefficient K_c does not depend on the shelf temperature (Equation 5) and thus has
400 a constant contribution in K_v for all the temperatures tested. The radiative coefficient K_r
401 depends on the third power of the shelf temperature and increases by about 1 $W\ m^{-2}\ K^{-1}$
402 between -25 °C and 25 °C for all pressures considered. The gas conduction coefficient K_g
403 depends on the gas temperature and decreases by 0.1-0.2 $W\ m^{-2}\ K^{-1}$ at low pressures (4-6
404 Pa) and by 1.1 $W\ m^{-2}\ K^{-1}$ at 50 Pa, between the two considered values of shelf temperature.
405 When increasing shelf temperature, the increase of K_r is partly compensated by the decrease
406 of K_g. These results confirm that the dependence of K_v on the shelf temperature is negligible,
407 especially if compared with the role played by the chamber pressure. Pisano et al.[12] and
408 Hottot et al.[23] reported similar K_v values for different shelf temperature conditions.
409
410 **Inter-vial heat transfer heterogeneity and the role of vial dimensions**
411 Figure 5 presents the experimentally observed distributions of the vial heat transfer
412 coefficient data of central vials at six chamber pressures. Since temperature- and equipment-
413 induced variations were minor, data obtained in LYO A and B and for the two shelf
414 temperatures were merged. A significant variability in the K_v values evaluated for central
415 vials was observed, the standard deviation increasing with pressure from 0.84 to
416 2.46 $W\ m^{-2}\ K^{-1}$. The values of standard deviation corresponded to coefficient of variation
417 comprised between 4 and 8 % depending on the operating conditions. The measurement error
418 associated to the determination of K_v was evaluated as the sum of the individual
419 measurement accuracy of each parameter entering in the calculation of K_v (Equation 1). The
420 measurement uncertainty was estimated to be ~ 1 %. This value is in agreement with the
421 value reported by Pikal et al.[5], who reported an uncertainty value of ~1.2 %. The
422 measurement uncertainty alone did not allow to completely explain the variability of the K_v

423 data. An external factor responsible for inter-vial heat transfer heterogeneity had thus to be
424 considered.
425 Attention was focused on the container: the geometrical difference among the vials was
426 considered as a possible source of the heat transfer heterogeneity. This variability in the vial
427 dimensions can be due to production limits and could change as a function of the container
428 model and provider. For the tested vial set, the coefficient of variation was approximately
429 27.7 % for the mean bottom curvature depth (l) and 23.9 % for the imprint-based contact area
430 (A_c). Hence, the effect of the variability of these geometrical dimensions on K_v was evaluated
431 as proposed in the Theory and data analysis section using the set of coefficients C reported in
432 Table 2.
433 Figure 6 displays the simulated distributions of K_v based on the vial bottom dimensions.
434 These distributions showed a trend and range of K_v values similar to the experimental ones.
435 At low pressure, K_v variability is almost completely due to the contact area variability. The
436 importance of the contact area on the K_v value was also confirmed by Pikal et al.[5] and
437 Cannon et al.[16] Regarding the vial bottom curvature, the importance of its variability
438 increased when the pressure rose. This is due to the coefficient K_g that plays a major role in
439 the total value of K_v at 40 and 50 Pa, as shown in Figure 3. The role of the bottom curvature
440 dimension was previously investigated by Brülls and Radsmuson[15] and Cannon et al.[16] Brülls
441 and Radsmuson[15] have shown that the bottom curvature has an impact on the heat transfer
442 only at chamber pressures higher than 30 Pa. This conclusion was confirmed by Cannon et
443 al.[16], who found that bottom curvature had little impact when considering low pressure (< 27
444 Pa). Our results agree with these conclusions,[15,16] confirming that the variability of the
445 bottom curvature depth has to be taken into consideration only if cycles at high chamber
446 pressure are performed (> 30 Pa).

Figure 7 displays the coefficient of variation of the experimental and calculated K_v distributions at different pressures. For the experimental distributions, the coefficient was calculated as an average between the LYO A and B datasets. The trend of the observed coefficient of variations for both experimental and simulated K_v distributions decreased from approximately 9 % to 4 % when increasing the chamber pressure. The variability of the experimental K_v distributions is completely explained by the geometrical variability at low pressures (i.e., 4, 6 Pa), whereas at higher pressures, the experimental coefficient of variation appears to be slightly higher than the one calculated based on vial geometry. It is thus possible that other sources of variability should be taken into consideration, for example convection in the drying chamber could play a role if higher pressures are considered.[22]

These considerations can guide the selection of the container as a function of the variability of the vial dimensions. The results obtained show that at low chamber pressure (i.e., 4, 6, 9, 15 Pa), it is important to assess the variability of the contact area between the vial and the shelf, whereas for cycles performed at high pressure (i.e., 40, 50 Pa), the variability of the bottom curvature depth becomes a relevant parameter. Consequently, for pharmaceutical processes that are usually carried out at pressures lower than 10 Pa, the contact area needs to be taken into account more than the bottom curvature depth.

Impact of K_v heterogeneity on the product temperature distribution within a batch of vials located in the centre of the shelf and not exposed to edge effect

In the case of freeze-drying, product temperature is one of the most important critical quality parameters. During the process, product temperature must be maintained close to a limit value (i.e., glass transition temperature for amorphous products, T_g) in order to optimize the process time but not to exceed it so as to guarantee the visual aspect of the cake and the product quality.

The vial-to-vial heat and mass transfer heterogeneity during the sublimation step causes variability in the product temperature. Considering a constant and fixed value of mass transfer resistance, it would be interesting to estimate the product temperature distribution during the primary drying step resulting only from the variability in vial geometry. Product temperature distributions were thus evaluated considering the contact area and curvature-based K_v distributions. For this analysis, a 5 % w/w sucrose solution was considered, processed at -25 °C and four different pressures (4, 6, 9 and 15 Pa). Relevant data concerning product resistance and glass transition temperature (-32 °C) were found in the literature.[21] As expected, product temperature increased from 4 Pa to 15 Pa because of the higher value of the vial heat transfer coefficient and higher ice sublimation temperature.

The variability of the product temperature was estimated to be approximately 0.9 °C at 15 Pa and as large as 2.2 °C at 4 Pa, considering ± 3 times the standard deviation that includes 99 % of the vials (Figure 8). A practical implication of these results is that, at the low pressures commonly encountered in vaccine freeze-drying, a temperature safety margin of approximately 2 °C has to be considered with respect to cycles designed on the basis of an average K_v value and to vials not exposed to edge effect.

Vials located at the periphery of the shelf (i.e., edge vials) receive additional heating due to the radiation from the chamber walls and the contact with the metallic guardrail. Thus, edge vials present a higher sublimation rate and a higher product temperature respect central vials.[5] Tang et al.[24] reports that the temperature difference between edge vials and central vial can be up to 2 °C at a shelf temperature of 20 °C and up to 4 °C at -30 °C for a chamber pressure of about 10 Pa. Depending on the operating conditions of the process, the safety product temperature margin resulting from variability in vial dimensions could be in the same order of magnitude than the safety margin imposed by the "edge effect".

CONCLUSIONS

Implementation of the Quality by Design initiative require a precise definition of the acceptable range for all product and process variables ensuring the fulfillment of the critical quality attributes of the final product. The impact of any variation of these variables on the final quality need to be quantified in advance. In this work, the effect of the variability of geometrical dimensions observed within a batch of vials (i.e., contact area between the shelf and the vial and the mean bottom curvature depth) on product quality was explored. The product quality was evaluating by predicting the product temperature knowing the vial heat transfer coefficient K_v. An original approach was proposed to calculate K_v distribution based on geometrical dimensions when considering a batch of vials located in the center of the shelf not exposed to any edge effect. The impact of freeze-dryer configuration and operating conditions was also considered. When considering low pressure (< 10 Pa), commonly used for freeze-drying biopharmaceuticals, the influence of freeze-dryer configuration and shelf temperature on heat transfer characteristics can be neglected and K_v distribution is completely explained by the contact area distribution. Furthermore the variability of vial dimension results in the definition of a product temperature safety margin of 2 °C. However, additional sources of variability need to be included in QbD approach. In particular, a study focused on the variability between edge and central vials and its role in cycle scale-up is presently ongoing.

ACKNOWLEDGMENTS

The authors would like to thank Benoit Moreau and Yves Mayeresse (GSK Vaccines) for reviewing this manuscript and Vincent Ronsse (technician) and Alain Philippart (operator) (GSK Vaccines) for their help in the data acquisition.

CONFLICT OF INTEREST

Erwan Bourlés is an employee of the GSK group of companies. Bernadette Scutellà participated in a postgraduate PhD program at GSK Vaccines. Stephanie Passot, Fernanda Fonseca and Ioan Cristian Trelea report no financial conflicts of interest.

FUNDING

This work was funded by GlaxoSmithKline Biologicals S.A., under a Cooperative Research and Development Agreement with INRA (Institut National de la Recherche Agronomique) via the intermediary of the UMR (Unité Mixte de Recherche) GMPA (Génie et Microbiologie des Procédés Alimentaires) at the INRA Versailles-Grignon research center.

AUTHORS' CONTRIBUTIONS

Bernadette Scutellà, Stephanie Passot, Erwan Bourlés, Fernanda Fonseca and Ioan Cristian Trelea were involved in the conception and design of the study. Bernadette Scutellà and Erwan Bourlès acquired the data. Bernadette Scutellà, Stephanie Passot, Erwan Bourlès, Fernanda Fonseca and Ioan Cristian Trelea analyzed and interpreted the results. All authors were involved in drafting the manuscript or revising it critically for important intellectual content. All authors had full access to the data and approved the manuscript before it was submitted by the corresponding author.

APPENDIX

The evaluation of the mean bottom curvature depth l was performed from geometrical considerations on the semi-spherical calotte at the vial bottom, as represented in Figure A. The bottom curvature depth depends on the radius of the vial bottom as follows:

$$l(r) = R_c - a(r) \qquad \text{Equation A1}$$

where R_c is the radius of the calotte and $a(r)$ is the distance between the shelf and the vial bottom, measured normal to the vial bottom:

$$a(r) = \sqrt{(R_c - l_{max})^2 + r^2} \qquad \text{Equation A2}$$

R_c can be calculated as a function of the maximum bottom curvature depth l_{max} and the inner vial bottom radius R_i:

$$R_c^2 = R_i^2 + (R_c - l_{max})^2 \qquad \text{Equation A3}$$

The area-mean bottom curvature depth can be defined as the integral of $l(r)$ on the calotte, divided by the area:

$$l = \frac{1}{A}\int l(r)\, dA \qquad \text{Equation A4}$$

The relevant area for heat transfer by gas conduction is:

$$A = \pi\, R_i^2 \qquad \text{Equation A5}$$

and the area element:

$$dA = 2\pi\, r dr \qquad \text{Equation A6}$$

Combining Equations A1-A6, l was calculated as:

$$l = \frac{2}{R_i^2}\int_0^{R_i}(R_c - \sqrt{(R_c - l_{max})^2 + r^2}\,)\, r\, dr \qquad \text{Equation A7}$$

REFERENCES

1. Jennings TA. 1999. Lyophilization: introduction and basic principles. Englewood, CO: Interpharm Press.
2. Nail SL, Searles JA. 2008. Elements of quality by design in development and scale-up of freeze parenterals. Biopharm Int 21(1):44–52.
3. Franks F. 1998. Freeze-drying of bioproducts: putting principles into practice. Eur J Pharm Biopharm 45:221–229.
4. Hibler S, Wagner C, Gieseler H. 2012. Vial Freeze-Drying, part 1: New Insights into Heat Transfer Characteristics of Tubing and Molded Vials. J Pharm Sci 101(3):1189–1201.
5. Pikal MJ, Roy ML, Shah S. 1984. Mass and heat transfer in vial freeze-drying of pharmaceuticals: role of the vial. J Pharm Sci 73(9):1224–1237.
6. Johnson R, Lewis L. 2011. Freeze-drying protein formulations above their collapse temperatures: possible issues and concerns. Am Pharm Rev 14(3):50–54.
7. Hibler S, Gieseler H. 2012. Heat transfer characteristics of current primary packaging systems for pharmaceutical freeze-drying. J Pharm Sci 101(11):4025–4031.
8. Pikal MJ. 2000. Heat and mass transfer in low pressure gases: applications to freeze drying. In Drugs and the Pharmaceutical Sciences 102:611–686.
9. Rambhatla S, Pikal MJ. 2003. Heat and mass transfer scale-up issues during freeze-drying, I: atypical radiation and the edge vial effect. Aaps Pharmscitech 4(2):22–31.
10. Pisano R, Fissore D, Barresi AA, Brayard P, Chouvenc P, Woinet B. 2013. Quality by design: optimization of a freeze-drying cycle via design space in case of heterogeneous drying behavior and influence of the freezing protocol. Pharm Dev Technol 18(1):280–295.

600 11. Pikal MJ, Bogner R, Mudhivarthi V, Sharma P, Sane P. 2016. Freeze-Drying Process
601 Development and Scale-Up: Scale-Up of Edge Vial Versus Center Vial Heat Transfer
602 Coefficients, Kv. J Pharm Sci doi:10.1016/j.xphs.2016.07.027.
603 12. Pisano R, Fissore D, Barresi AA. 2011. Heat Transfer in Freeze-Drying Apparatus. In:
604 Dos Santos Bernardes MA ed., Developments in Heat Transfer 91-114. Rijeka, Croatia:
605 InTech. Available from: http://www.intechopen.com/books/developments-in-heat-
606 transfer/heat-transfer-infreeze-drying-apparatus.
607 13. Nail SL. 1980. The Effect of Chamber Pressure on Heat Transfer in the Freeze Drying of
608 Parenteral Solutions. PDA J Pharm Sci Technol 34(5):358–368.
609 14. Ybema H, Kolkman-Roodbeen L, te Booy MP, Vromans H. 1995. Vial lyophilization:
610 calculations on rate limitation during primary drying. Pharm Res 12(9):1260–1263.
611 15. Brülls M, Rasmuson A. 2002. Heat transfer in vial lyophilization. Int J Pharm 246(1-
612 2):1–16.
613 16. Cannon A, Shemeley K. 2004. Statistical evaluation of vial design features that influence
614 sublimation rates during primary drying. Pharm Res 21(3):536–542.
615 17. Kuu WY, Nail SL, Sacha G. 2009. Rapid determination of vial heat transfer parameters
616 using tunable diode laser absorption spectroscopy (TDLAS) in response to step-changes
617 in pressure set-point during freeze-drying. J Pharm Sci 98(3):1136–1154.
618 18. Monchau JP, Marchetti M, Ibos L, Dumoulin J, Feuillet V, Candau Y. 2014. Infrared
619 Emissivity Measurements of Building and Civil Engineering Materials: A New Device
620 for Measuring Emissivity. Int J Thermophys 35:1817-31.
621 19. Trelea IC, Passot S, Fonseca F, Marin M. 2007. An Interactive Tool for the Optimization
622 of Freeze-Drying Cycles Based on Quality Criteria. Dry Technol 25(5):741–751.
623 20. Bird RB, Stewart WE, Lightfoot EN. 1960. Transport phenomena. New York, NY: John
624 Wiley & Sons.

21. Konstantinidis AK, Kuu W, Otten L, Nail SL, Sever RR. 2011. Controlled nucleation in freeze -drying: Effec
and primary drying rate. J Pharm Sci 100(8):3453–3470.
22. Ganguly A, Nail SL, Alexeenko A. 2013. Experimental Determination of the Key Heat Transfer Mechanisms in Pharmaceutical Freeze-Drying. J Pharm Sci 102(5):1610–1625.
23. Hottot A, Vessot S, Andrieu J. 2005. Determination of mass and heat transfer parameters during freeze-drying cycles of pharmaceutical products. PDA J Pharm Sci Technol 59(2): 138–153.
24. Tang X, Nail SL, Pikal MJ. 2006. Evaluation of manometric temperature measurement, a process analytical technology tool for freeze-drying: Part I, product temperature measurement. AAPS PharmSciTech 7(1):E95–E103.

638 **FIGURES**

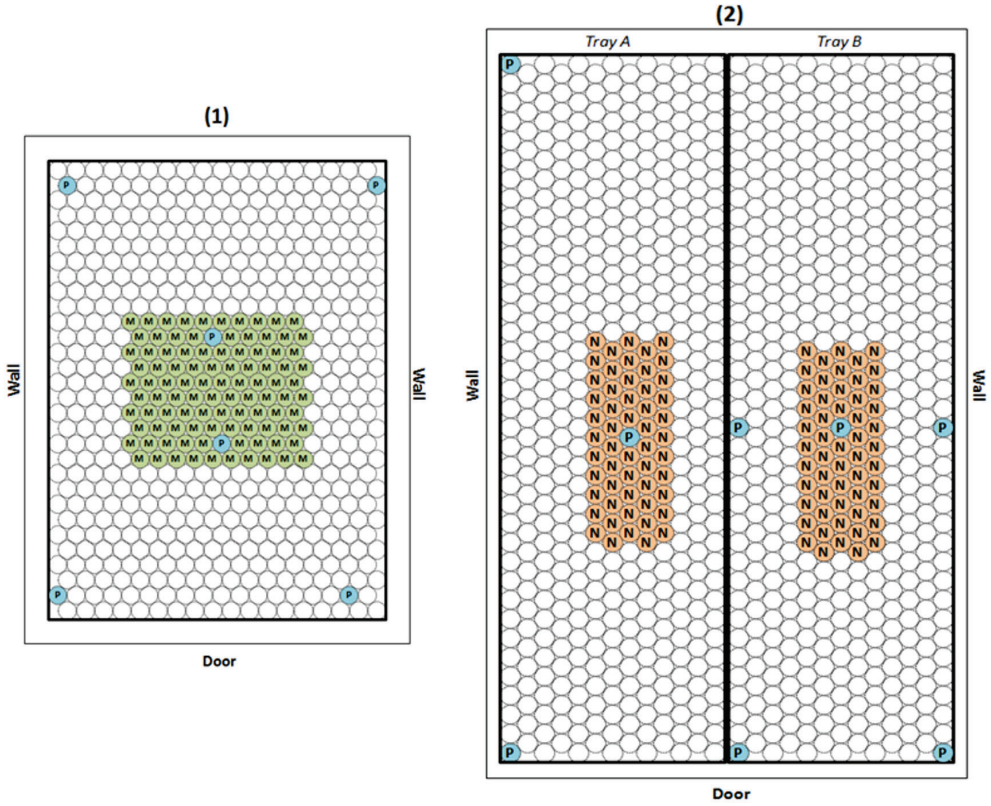

639

640 **Figure 1.** Vial arrangements in (1) LYO A and (2) LYO B. Gravimetrically-analyzed vials
641 are marked with the letters M and N for LYO A and B, respectively. Vials in which wireless
642 temperature probes were located are marked with the letter P. All vials were filled with 1.8
643 mL of pure water.

644

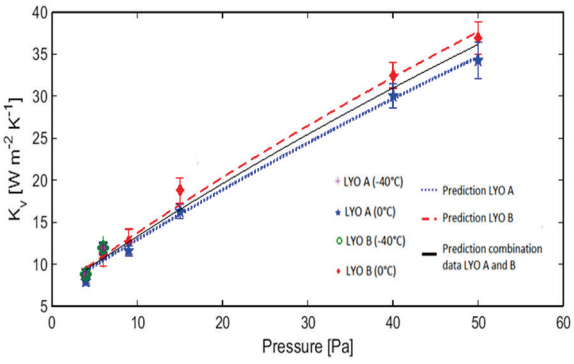

645

Figure 2. Vial heat transfer coefficient (K_v) values vs. chamber pressure (P_c). The markers refer to the K_v average values measured in LYO A and B at -40°C and 0°C. The lines correspond to the values calculated with Equation 14 with the data obtained from LYO A, B and their combination. Error bars represent standard deviations.

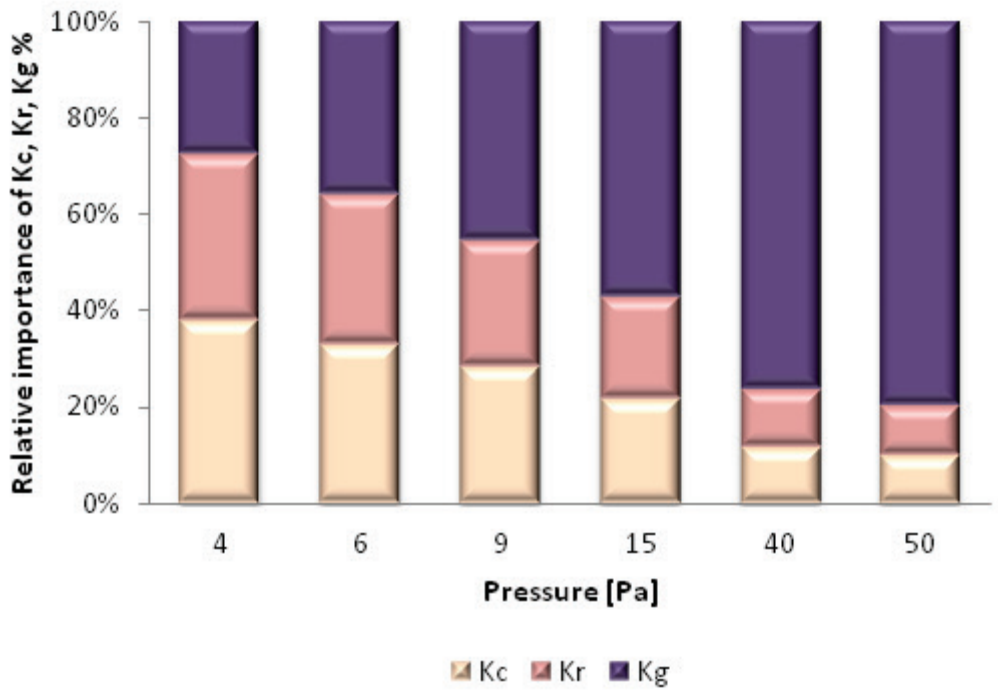

Figure 3. Relative importance of the heat transfer coefficients by contact conduction (K_c), radiation (K_r) and conduction through the gas (K_g) as percentages of the total heat transfer coefficients (K_v). Average values of the contact area (A_c) and mean bottom curvature depth (l) were considered in this calculation. The set of coefficients C (Table 2) was used to evaluate K_c and K_g.

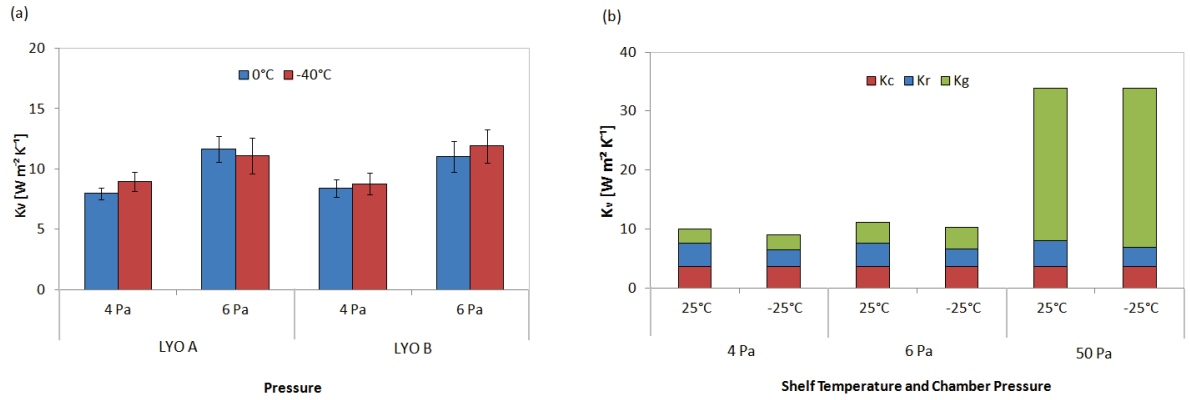

658

659 **Figure 4.** Influence of the shelf temperature on the vial heat transfer coefficients K_v. K_v
660 values were evaluated at different shelf temperatures and chamber pressures (a) from
661 experimental data obtained in LYO A and B and (b) from the coefficients K_c, K_r and K_g,
662 calculated using Equations 5, 6 and 10.

663

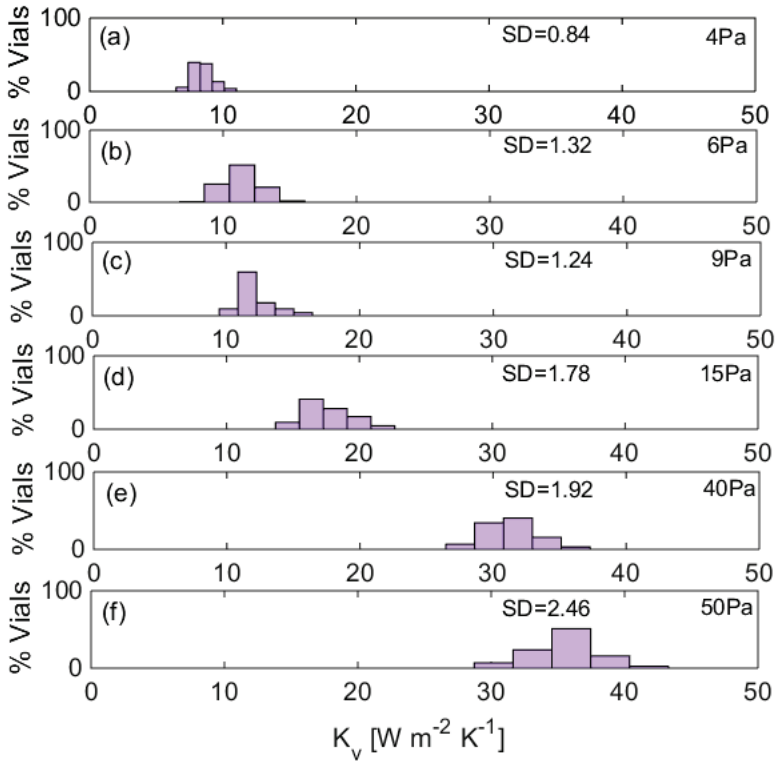

664

665 **Figure 5.** Experimentally-measured distribution of the vial heat transfer coefficients at 4 Pa
666 (a), 6 Pa (b), 9 Pa (c), 15 Pa (d), 40 Pa (e) and 50 Pa (f). Data of LYO A and LYO B at
667 different shelf temperatures (0°C and -40°C) were combined.

668

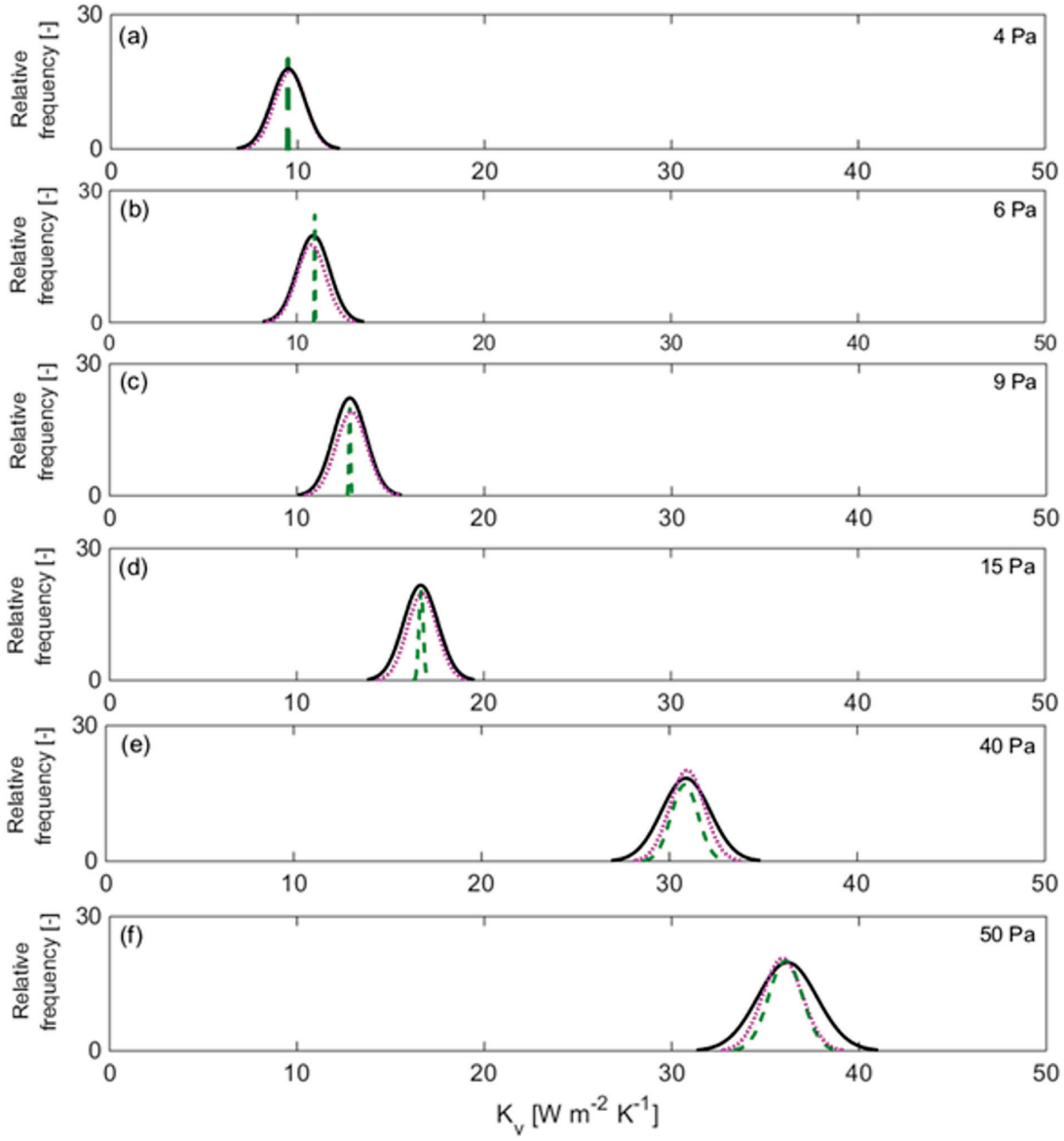

669

670 **Figure 6.** Calculated K_v normal distributions: curvature-based (dashed green line – –),
671 contact area-based (dotted red line - - -) and combined curvature and contact area-based
672 (solid black line —) at 4 Pa (a), 6 Pa (b), (c) 9 Pa (c), 15 Pa (d), 40 Pa (e) and 50 Pa (f).

673

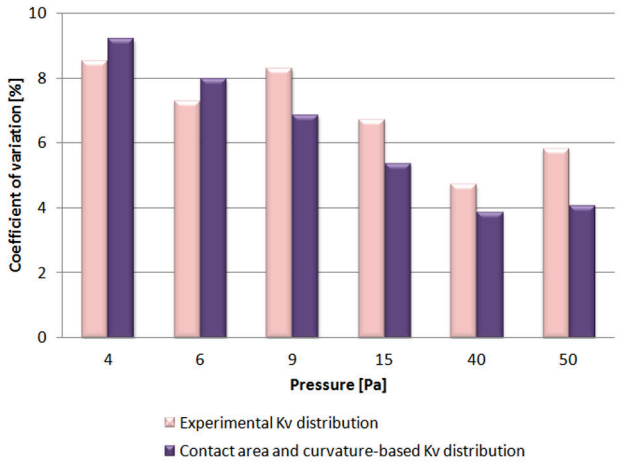

674

675 **Figure 7.** Coefficients of variation of experimentally-measured K_v distribution (LYO A and
676 B; light bars) and calculated (combined contact area and curvature-based) K_v distribution
677 (dark bars) and at different pressures.

678

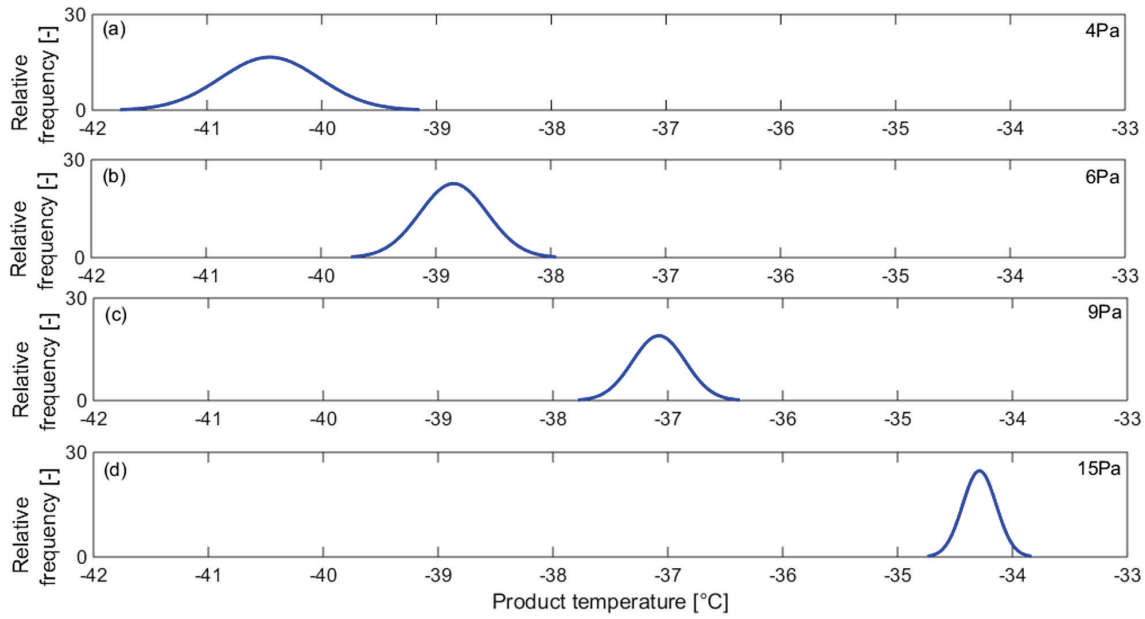

679

680 **Figure 8.** Product temperature distributions obtained from the contact area and curvature-
681 based distribution for a 5 % w/w sucrose solution processed at a shelf temperature of -25 °C
682 and four chamber pressures: (a) 4 Pa, (b) 6 Pa, (c) 9 Pa and (d) 15 Pa.

683

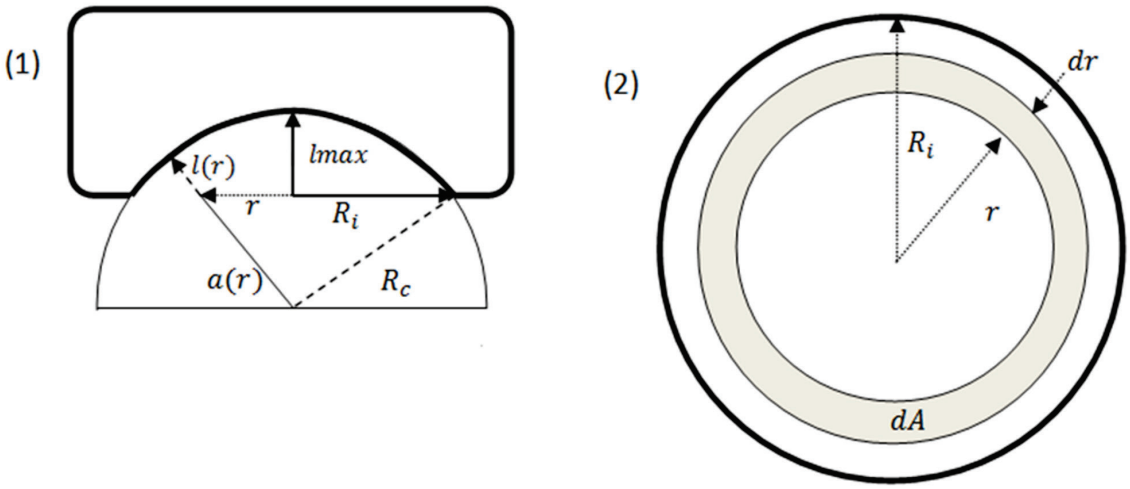

684

685 **Figure A.** Side (1) and top (2) view of the vial bottom represented as a semi-spherical calotte.

686

687

688